Transverse dichotomic ratchet in a two-dimensional corrugated channel

Pavol Kalinay
Institute of Physics, Slovak Academy of Sciences, Dúbravska cesta 9, 84511, Bratislava, Slovakia

(Received 29 June 2022; accepted 23 September 2022; published 17 October 2022)

A particle diffusing in a two-dimensional channel of varying width $h(x)$ is considered. It is driven by a force of constant magnitude f, but random orientation across the channel. We suggest the projection technique to study the ratchet effect appearing in this system. Reducing the transverse coordinate, as well as the orientation of the force in the full-dimensional Fokker-Planck equation, we arrive at the generalized Fick-Jacobs equation, describing dynamics of the system in the longitudinal coordinate x only. The additional effective potential $-\gamma(x)$, calculated within the mapping procedure, exhibits an increasing or decreasing part in the channel shaped by an asymmetric periodic $h(x)$, which determines the appearing ratchet current. As shown on a specific example, random driving in the transverse direction is much more effective than that in the longitudinal direction, at least for quickly flipping orientation of the force. Also, the transverse and the longitudinal driving push the rectified current in opposite directions along the same channel.

DOI: 10.1103/PhysRevE.106.044126

I. INTRODUCTION

One of the mechanisms keeping the world moving instead of its decay in the thermodynamic equilibrium, is rectification of the stochastic motion of a diffusing particle (or a system represented by a point in the space of relevant parameters). To avoid approaching the equilibrium, the particle has to be driven by some source of energy, which usually does not prefer any specific direction. Nevertheless, the net motion becomes finally rectified due to asymmetric confinement, working as a ratchet. There are many ways to drive the system out of equilibrium and rectify its motion, which enables us to specify various classes of ratchets [1,2].

Anyway, the detailed analysis of such systems is rather complicated, especially because of interaction of the driven particle with a nontrivial confinement, resulting in the ratchet effect. Recently, an idea of applying the dimensional reduction for the Feynman-Smoluchowski (FS) ratchet was introduced [3–5]. The two-dimensional (2D) Fokker-Planck equation describing the stochastic motion of the system was projected onto the "reaction" coordinate x (rotation of the wheel). After integration over the "transverse" coordinate (position of the pawl), the interaction with confinement is involved in the structure of the resulting mapped 1D generalized Fick-Jacobs (FJ) [6] equation, which noticeably simplifies the next analysis.

Another system which can be studied by a similar procedure are the active particles [7,8] in a confinement. Aside from diffusion, they are self-propelled by some force of a (roughly) constant magnitude in a direction depending on their orientation. The particles stochastically rotate, so the direction of the force is random. Unlike the FS ratchet, the active particles reflect real experiments. They can represent, e.g., bacteria [9], or they are prepared artificially as the Janus particles [10,11], having platinum spots on their surfaces. If immersed in the solution of H_2O_2, Pt catalyzes its decomposition, which pushes the particles in the opposite direction. The experiments [12–14] as well as the numerical simulations [15–21] show that the active particles placed in an asymmetric confinement exhibit either violation of their equilibrium distribution or rectification of their motion.

The theoretical analysis of the ratchet effect in such systems [22–27] requires us to study correlations of motion of particles in particular directions near the boundary. In the simplest case of active disks placed in a corrugated two-dimensional (2D) channel, we have to consider driven diffusion in two spatial coordinates and the third one, orientation of the disk, determining the direction of the self-propulsion. It is still a rather complicated task, so other simplifications are introduced. Diffusion in the 2D channel of varying width $h(x)$ is often approximated by 1D diffusion along the longitudinal coordinate x in the entropic potential $U_{\rm en}(x) = -\ln h(x)$. Consistently, only two possible orientations remain in this reduced 1D picture, with the random force acting forward or backward along the channel. This model can also describe a passive particle driven by the random dichotomic force.

Dichotomy of the random force represents one of the simplest possible ways to drive the system (the diffusing particle) out of equilibrium. It results in a nonzero rectified current in asymmetric periodic potentials, described as the fluctuating force ratchet [1,28,29]. Recently, we showed [30] that the projection technique similar to that used in a FS ratchet can also be effectively applied to study this simple ratchet model.

The projection technique was originally developed for diffusion in 2D (or 3D) channels of varying cross sections, which is reduced to a 1D description working in the only spatial coordinate x. The method is based on scaling of the transverse coordinate(s) by a small auxiliary parameter $\sqrt{\epsilon}$, (or the transverse diffusion constant, becoming $\sim 1/\epsilon$), which makes the diffusion across the channel very fast. In the limit $\epsilon \to 0$, the transverse profile of the particle's density becomes

flat, which leads to the FJ equation [6] after integration of the 2D or 3D diffusion equation over the cross section. A slower transverse relaxation for $\epsilon > 0$ deflects the transverse profile from the uniform distribution, depending on the shape of the boundaries and the flux. Calculating these deviations, the projection technique [31,32] enables us to derive recursively the corrections $\hat{Z}_n$ to the FJ equation controlled by ϵ,

$$\partial_t p(x,t) = D_0 \partial_x A(x)[1 - \hat{Z}(x,\partial_x)]\partial_x \frac{p(x,t)}{A(x)};$$
$$\hat{Z}(x,\partial_x) = \sum_{n=1}^{\infty} \epsilon^n \hat{Z}_n(x,\partial_x), \tag{1.1}$$

which can be simplified in the form

$$\partial_t p(x,t) = \partial_x A(x) D(x) \partial_x \frac{p(x,t)}{A(x)} \tag{1.2}$$

for almost the stationary transport [32–35]. Both equations govern the marginal 1D density $p(x,t)$, $A(x)$ stands for $h(x)$ in 2D or the cross section area in 3D channels. D_0 denotes the intrinsic diffusion constant, which is replaced by the spatial-dependent effective diffusion coefficient $D(x)$ in Eq. (1.2), calculated directly from the correction operators $\hat{Z}_n(x,\partial_x)$.

In the 1D dichotomic ratchet, the role of the scaling parameter ϵ is played by inverse of the rate α of flipping between the two orientations of the force [30]. The only transverse coordinate here is orientation of the force. In the case of infinite α, the flipping is so fast that the probability that the particle is driven there or back is the same, independent of its position x, hence we obtain the Smoluchowski equation for the net 1D density $p(x,t)$. For a slower flipping, the particle has a time to react whether it is pushed uphill or downhill before the next flip of the force, so the local densities of particles driven in the opposite directions start to differ from one another. This is reflected by the mapping procedure, which generates a series of corrections to the zeroth order Smoluchowski equation in the same way as $\hat{Z}_n$ in Eqs. (1.1), however, expanded now in $1/\alpha$. Also, $A(x)$ has a different meaning; it represents here the Botzmann weight of the 1D potential $U_{\rm en}(x)$ corrected by a series of additional contributions $\gamma_n(x)$, also controlled by $1/\alpha$, coming from the stochastic driving. Starting from the order $\sim\alpha^{-3}$, these terms exhibit nonzero increments over one period in asymmetric periodic channels; thus they visualize the effective force driving the rectified current.

Subsequently, the mapping procedure can be extended to the true 2D channel, where the particles are still driven by the randomly flipping longitudinal force only [36]. The method combines both scaling of the transverse coordinate y as well as the flipping rate α. The infinitely fast flipping together with infinitely fast transverse relaxation, controlled by the common parameter $\epsilon \to 0$, result in the FJ equation. A finite ϵ gives the particles driven there or back the time to react correspondingly at the curved boundary $y = h(x)$, biasing their local densities from $p(x,t)/2h(x)$ in a different way. The mapping involves these changes in the corrections $\hat{Z}_n$ and also $A(x)$, which is now $h(x)$ multiplied by the exponential of the additional effective potential $\gamma(x)$, appearing due to the stochastic driving. Again, its nonzero increment over one period indicates the ratchet effect. Its leading term for $\epsilon > 0$ is now $\sim 1/\alpha$, so the asymptotic of the rectified current in the real 2D channels considerably differs from predictions of the 1D reduced FJ approximation.

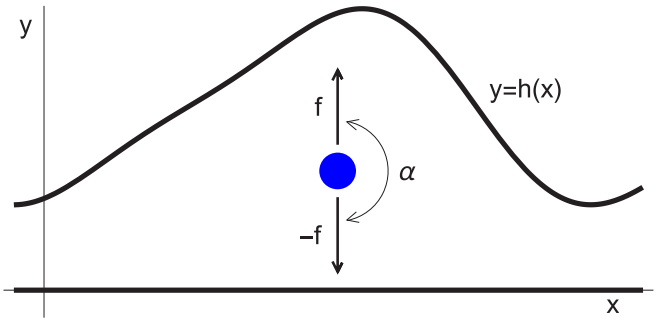

FIG. 1. Scheme of the ratchet driven by the transverse fluctuating force f in a 2D channel; α is the rate of the force flipping.

The next extension of the mapping to the full 2D Janus particle, rotating in an *arbitrary* angle in a nonhomogeneous channel, is not quite straightforward. Except for the particle's orientation aiming forward or backward along the channel, considered in previous works, the driving force f has a nonzero transverse component there, i.e., in the direction, which is reduced by the mapping. So we need to revise several steps of the mapping procedure in this case, namely, how to understand the FJ approximation, definition of the entropic potential, and then to derive the corrections, giving rise to the ratchet effect. To answer these nontrivial questions, we will study here a simplified model of a particle driven now by the fluctuating transverse force f, aiming only up or down, see Fig. 1. Still, it could also represent real systems, e.g., the dynamics of diffusing particles driven by the potential flipping randomly between the opposite walls of a nonhomogeneous channel.

Nevertheless, the aim of the presented paper is rather methodological: to derive the effective 1D description if the force driving the diffusing particle flips in the direction which is reduced. In Sec. II, we formulate mathematically the problem, find the FJ equation and its corrections in $1/\alpha$ for an infinitely fast diffusion across the channel, i.e., the 1D reduction of the model. In Sec. III, we develop the theory also including the finite speed of transverse relaxation. We demonstrate the appearance of the ratchet effect on a specific example of the periodic asymmetric channel (Fig. 1). The backward mapping, which is the key part of the projection method, enables us to visualize the distribution of 2D particle's density and currents and thus to analyze the mechanism of rectification.

Our model also brings interesting results if compared to the closely related previous model with the force flipping in the longitudinal direction [30,36]. A different orientation of the flipping force (with zero mean) exhibits a considerably different behavior of the ratchet effect in the same system. The transverse driving spins the whirls of diffusing particles in the opposite direction as the longitudinal one, resulting in opposite directions of the ratchet current, too.

II. SPATIAL FICK-JACOBS APPROXIMATION

First, we formulate the model to be solved. The particles are diffusing in a 2D channel bounded by the x axis and an

analytic function $y = h(x) > 0$. The flipping force f drives them randomly upward or downward, see Fig. 1. Regardless of its origin, we can consider two types of the particles, pushed up (+) or down (−), converting to one another with the rate constant α. Their 2D probability densities $\rho_\pm(x, y, t)$ obey the Smoluchowski equations for the transverse forces $\pm f$, coupled by the reaction term $\sim\alpha$, describing the flipping

$$\partial_t \rho_\pm(x, y, t) = D_0\left[\partial_x^2 + \frac{1}{\epsilon}\partial_y(\partial_y \mp f)\right]\rho_\pm(x, y, t) \mp \alpha[\rho_+(x, y, t) - \rho_-(x, y, t)]. \quad (2.1)$$

We will work in units where the temperature $k_BT = 1$ and also the diffusion constant $D_0 = 1$. The scaling of the transverse diffusion constant by a small auxiliary parameter ϵ, necessary for the mapping method, is already included here. The no-flux boundary conditions (BCs) at $y = 0$ and $y = h(x)$ are supplemented for both orientations,

$$(\partial_y \mp f)\rho_\pm(x, y, t)|_{y=h(x)} = \epsilon h'(x)\partial_x\rho_\pm(x, y, t)|_{y=h(x)}, \quad (\partial_y \mp f)\rho_\pm(x, y, t)|_{y=0} = 0; \quad (2.2)$$

the prime denotes the derivative according to x.

We start with reduction of the transverse coordinate y, following the same steps as for diffusion driven by the transverse force [37], separately for each orientation. Integrating Eqs. (2.1) over the cross section and applying BCs (2.2), we arrive at the coupled equations

$$\partial_t p_\pm(x, t) = D_0\partial_x[\partial_x p_\pm(x, t) - h'(x)\rho_\pm(x, h(x), t)] \mp \alpha[p_+(x, t) - p_-(x, t)], \quad (2.3)$$

governing the marginal densities of (+) and (−) particles:

$$p_\pm(x, t) = \int_0^{h(x)} \rho_\pm(x, y, t)dy. \quad (2.4)$$

To close the equations, we still need to express the 2D densities $\rho_\pm(x, y, t)$ at the boundary $y = h(x)$ using the 1D densities $p_\pm(x, t)$. The 2D densities $\rho_{\pm0}(x, y, t)$ in the FJ approximation are obtained in the limit $\epsilon \to 0$. Elimination of the diverging terms $\partial_y(\partial_y \mp f)\rho_{\pm0} = 0$ of Eq. (2.1) requires

$$\rho_{\pm0}(x, y, t) = \frac{fe^{\pm f[y-h(x)/2]}}{2\sinh[fh(x)/2]}p_\pm(x, t), \quad (2.5)$$

also satisfying the definition (2.4) and BC $(\partial_y \mp f)\rho_{\pm0} = 0$ at $y = 0$ and $h(x)$. These solutions express immediate transverse equilibration of both types of particles due to infinite transverse diffusion constant D_0/ϵ. Applying them in Eq. (2.3), we obtain the spatial FJ approximation for particular orientations:

$$\partial_t p_\pm(x, t) = \partial_x\left[\partial_x - \frac{fh'(x)e^{\pm fh(x)/2}}{2\sinh[fh(x)/2]}\right]p_\pm(x, t) \mp \alpha[p_+(x, t) - p_-(x, t)]. \quad (2.6)$$

However, our aim is to find the equation for the total 1D density:

$$p(x, t) = p_+(x, t) + p_-(x, t). \quad (2.7)$$

Summing Eq. (2.6) over both orientations, we get

$$\partial_t p(x, t) = \partial_x\left[\partial_x p(x, t) - \frac{fh'(x)}{2\sinh[fh(x)/2]} \times (e^{fh(x)/2}p_+(x, t) + e^{-fh(x)/2}p_-(x, t))\right], \quad (2.8)$$

where we need again to express $p_\pm(x, t)$ using $p(x, t)$. Similar to mapping the dichotomic ratchet driven by the longitudinal force [30], the necessary small parameter here is $\sim 1/\alpha$. In the limit of high flipping rate, the densities $p_\pm$ become equal, $p_+(x, t) = p_-(x, t) = p(x, t)/2$. If it is substituted in Eq. (2.8), we obtain the mapped equation in the FJ form

$$\partial_t p(x, t) = \partial_x\left[\partial_x - \frac{fh'(x)}{2}\coth\frac{fh(x)}{2}\right]p(x, t) = \partial_x A_0(x)\partial_x\frac{p(x, t)}{A_0(x)}, \quad (2.9)$$

where

$$A_0(x) = \frac{2}{f}\sinh\frac{fh(x)}{2}. \quad (2.10)$$

A_0 can be multiplied by any constant; Eq. (2.10) provides $A_0(x) \to h(x)$ in the limit of zero force f. Its minus logarithm is then the corresponding entropic potential.

Notice that in the FJ approximation, the transverse distributions of (+) and (−) particles are exponential according to Eq. (2.5), even for $\alpha \to \infty$. The transverse equilibration here is always faster than the flipping, protecting the profile to be flatten. A different approach considering the scaled α is presented in Sec. III.

Similar to the longitudinal driving, a slower flipping leaves the particle coming to x from the neighboring positions $x \pm dx$ of a different width in an unbalanced (previous) orientation for some time $\sim 1/\alpha$. The densities $p_\pm(x, t)$ start to deflect from $p(x, t)/2$, the deviations can be formally expressed using an operator $\hat\omega$ [30]:

$$p_\pm(x, t) = A(x)\left[\frac{1}{2} \pm \hat\omega(x, \partial_x)\right]\frac{p(x, t)}{A(x)}. \quad (2.11)$$

Introducing $A(x) = e^{\gamma(x)}A_0(x)$ here enables us to bring the final mapped equation in the form of Eqs. (1.1). $\gamma(x)$ is a gauge function, which will be fixed within the recurrence mapping procedure. Notice that the relation (2.11) keeps the definition (2.7) consistent. If it is substituted in Eq. (2.8), we arrive at

$$\partial_t p(x, t) = \partial_x A(x)[\partial_x + \gamma'(x) - fh'(x)\hat\omega(x, \partial_x)]\frac{p(x, t)}{A(x)} \quad (2.12)$$

after some algebra. As we see later, the operator $\hat\omega$ can be split into the part containing the derivatives ∂_x and just a function $\omega(x)$; $\hat\omega(x, \partial_x) = \tilde\omega(x, \partial_x)\partial_x + \omega(x)$. So we can convert Eq. (2.12) to the form (1.1) by setting

$$\gamma'(x) = fh'(x)\omega(x), \quad \hat Z(x, \partial_x) = fh'(x)\tilde\omega(x, \partial_x). \quad (2.13)$$

The key point of the mapping is fixing of the operator $\hat\omega$. Together with $\hat Z(x, \partial_x)$ and the function $\gamma(x)$, they represent the corrections to the zeroth order FJ Eq. (2.9), appearing there

due to a finite time $\sim 1/\alpha$ between the succeeding flips of the force. Thus, it is natural to express them as a series in $1/(2\alpha)$,

$$F(.) = \sum_{n=1}^{\infty} \frac{1}{(2\alpha)^n} F_n(.), \tag{2.14}$$

where F stands for $\hat{\omega}(x, \partial_x)$, $\hat{Z}(x, \partial_x)$, or $\gamma(x)$. We require the particular $p_\pm$, generated by the backward mapping relation (2.11), to satisfy Eq. (2.6) for any 1D solution $p(x, t)$. Having substituted there for $p_\pm$ and expressing the term $\sim 2\alpha$, we get

$$2\alpha\hat{\omega} = \frac{1}{A}\partial_x\left[\partial_x - \frac{fh'e^{fh/2}}{2\sinh(fh/2)}\right]A\left(\frac{1}{2} + \hat{\omega}\right) - \left(\frac{1}{2} + \hat{\omega}\right)\frac{1}{A}\partial_x A(1 - \hat{Z})\partial_x, \tag{2.15}$$

omitting writing the obvious arguments. The derivative ∂_t according to time commutes with all spatial operators to the right and the remaining $\partial_t p(x, t)$ is expressed using Eq. (1.1). The equation acts on any $p(x, t)/A(x)$, so it has to be satisfied on the level of operators.

If $\hat{\omega}$, $\hat{Z}$, and γ are expanded in $1/(2\alpha)$, Eq. (2.14), Eq. (2.15) generates the recurrence relations for $\hat{\omega}_n$, having completed the commutations on the right-hand side and collecting the terms of the same order. In the lowest zeroth order, we find

$$\hat{\omega}_1 = \frac{1}{2A_0}\partial_x^2 A_0 - \frac{1}{2A_0}\partial_x h' e^{fh/2} - \frac{1}{2A_0}\partial_x A_0 \partial_x = -\frac{fh'}{4}\partial_x - \frac{f}{4}\left[h'' + \frac{fh'^2}{2}\coth\frac{fh}{2}\right]. \tag{2.16}$$

We can easily identify the parts $\tilde{\omega}_1(x, \partial_x)$ and $\omega_1(x)$ here. Applying them in Eqs. (2.13), we obtain

$$\gamma_1' = -\frac{f^2 h'}{4}\left[h'' + \frac{fh'^2}{2}\coth\frac{fh}{2}\right], \qquad \hat{Z}_1 = -\frac{f^2 h'^2}{4}. \tag{2.17}$$

Collecting the terms $\sim 1/(2\alpha)$ in Eq. (2.15), we derive $\hat{\omega}_2$, yielding

$$\gamma_2' = -\frac{f^2 h'}{32}\left[f^3 h'^4\left(\frac{1}{\sinh^2(fh/2)} - 1\right)\coth(fh/2) - 2f^2 h'^2 h''\left(\frac{3}{\sinh^2(fh/2)} - 1\right) + 4f(2h''^2 + 3h'h^{(3)})\coth(fh/2) + 8h^{(4)}\right],$$

$$\hat{Z}_2 = \frac{f^2 h'}{16}\left[\frac{f^2 h'^3}{\sinh^2(fh/2)} - 8fh'h''\coth(fh/2) - 12h^{(3)} - 8h''\partial_x\right], \tag{2.18}$$

etc. The complexity of the formulas quickly grows with growing order; we derived them up to the fourth order by the computer algebra systems.

As seen in Eqs. (2.18), $\hat{Z}_2$ (as well as the higher coefficients $\hat{Z}_n$) contain the next derivatives ∂_x, which complicate us the use of Eqs. (1.1). So, it is simplified by Eq. (1.2), replacing the operator $(1 - \hat{Z})$ by a function $D(x)$, the effective diffusion coefficient. This equation is valid in the limit of stationary flow, i.e. when the time derivative of any quantity is negligible. In this limit, one can also find the relation

$$\frac{1}{D(x)} = A(x)[1 - \hat{Z}(x, \partial_x)]^{-1}\frac{1}{A(x)}, \tag{2.19}$$

enabling us to calculate $D(x)$ from the known coefficients $\hat{Z}_n$. Its derivation [30,32,36] is also described in the Appendix. Applying Eqs. (2.17) and (2.18) here, we find

$$\frac{1}{D(x)} = 1 - \frac{f^2 h'^2}{8\alpha} + \frac{f^2 h'}{64\alpha^2}[f^2 h'^3\coth^2(fh/2) - 4fh'h''\coth(fh/2) - 12h^{(3)}] + \ldots \tag{2.20}$$

up to the second order. We can easily check that the leading terms of all corrections $\sim f^2$, so they disappear when the driving is turned off. Then only the uncorrected FJ Eq. (2.9) with $A(x) = h(x)$ remains.

Equation (1.2) represents the 1D Smoluchowski equation with varying diffusion coefficient $D(x)$, hence the function $-\gamma(x)$ can be interpreted as an additional effective potential, extending the entropic potential $-\ln A_0(x)$ due to the stochastic driving. As we show later, integrating the derivatives $\gamma_n'(x)$, Eqs. (2.17), (2.18), etc., for a periodic asymmetric $h(x) = h(x + L)$, we can obtain a slanted washboard function, giving nonzero increment $\Delta\gamma = \gamma(L) - \gamma(0)$ over one period L. Then $\Delta\gamma/L$ represents the effective force driving the ratchet current J. Having the system described by Eq. (1.2), we can calculate the stationary current using the Stratonovich [38,39] or the Lifson-Jackson [40] formulas

$$J = \left(1 - e^{-\Delta\gamma}\right)\left[\int_0^L A(x)dx\int_x^{L+x}\frac{dx'}{A(x')D(x')}\right]^{-1} \simeq \Delta\gamma\left[\int_0^L A_0(x)e^{\gamma(x)}dx\int_0^L\frac{e^{-\gamma(x)}dx}{A_0(x)D(x)}\right]^{-1}, \tag{2.21}$$

(for small $\Delta\gamma$), modified by $D(x)$; see Appendix. One particle per period L is supposed.

We demonstrate our theory on the function

$$h(x) = 2 - \cos x + a\sin 2x, \tag{2.22}$$

described in Fig. 1. The parameter a regulates asymmetry of the channel; we used $a = 0.2$. Figure 2(a) describes the coefficients $\gamma_1(x)$ and $\gamma_2(x)$, calculated by numerical integration of the corresponding formulas (2.17) and (2.18) (from $x = 0$; the integration constants are irrelevant). Unlike the longitudinal driving [30], we observe nonzero contributions $\Delta\gamma_n = \gamma_n(2\pi)$ starting already from $n = 1$, so the asymptotic of the effective force driving the ratchet $\Delta\gamma/L \sim 1/\alpha$. Dependence of $\Delta\gamma$ on α is shown in Fig. 3 for $f = 1$ (solid) and $f = 2$ (dashed lines), taking the corrections up to the first, second, third, and fourth orders. As seen also in Fig. 2(a), $\Delta\gamma_n$ grows with growing n, so the obtained values are reliable only for higher α; roughly $\alpha > 5$ for this channel. Validity of the results is also restricted to smaller $f(< 2)$, i.e., for small persistence length $\sim f/\alpha$. $D(x)$ for the values $f = 1$, $\alpha = 5$, which are at the border of usability of the theory, are described in Fig. 2 b; the numbers assign the highest used order in the formula (2.20).

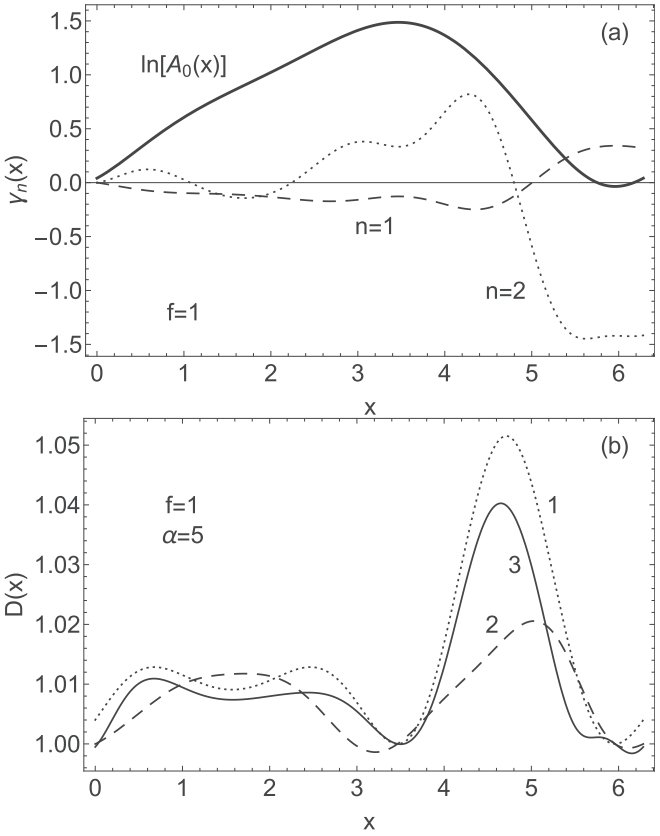

FIG. 2. (a) Coefficients $\gamma_1(x)$ (dashed) and $\gamma_2(x)$ (dotted) according to Eqs. (2.17) and (2.18) for $h(x)$ given by Eq. (2.22), $f = 1$, compared with the corresponding minus entropic potential (solid line). (b) Effective diffusion coefficient $D(x)$ for the same channel and driving; the flipping rate $\alpha = 5$. Dotted, dashed, and solid lines describe this function corrected up to the first, second, and third orders, respectively.

The driving increases $D(x)$ above unity in the style of the Taylor dispersion [28–30], but the corrections are tiny. Their influence to the ratchet current J, calculated according to Eq. (2.21), is negligible, at least in comparison with errors due to truncation of $\gamma(x)$. We used the simpler Lifson-Jackson formula to plot Fig. 4; the current is almost proportional to $\Delta\gamma$ ($\simeq 46J$ for our parameters). The solid lines describing the results taken up to nth order ($n = 1, .., 4$) are compared with the numerical solution (dots) of the stationary 1D problem, validating the mapping procedure for larger α. The dashed line depicts the ratchet current in the same channel driven by the longitudinal force of the same magnitude f [30,36]. Let us recall that $\Delta\gamma_n$ in that case becomes nonzero for $n \geqslant 3$, hence the asymptotic of $J_{\rm long} \sim 1/\alpha^3$. Let us stress that the currents flow in the opposite directions; the stochastic transverse force pushes the particles here to the right, while the longitudinal drives to the left.

The theory presented does not describe well the systems with a slowly flipping force. Still, knowing the mapping method described here, one can adapt an alternative scheme based on formulation of the differential equations for $\gamma(x)$ and $1/D(x)$, which avoid expansions in $1/\alpha$ [30]. This calculation exceeds the span of this paper.

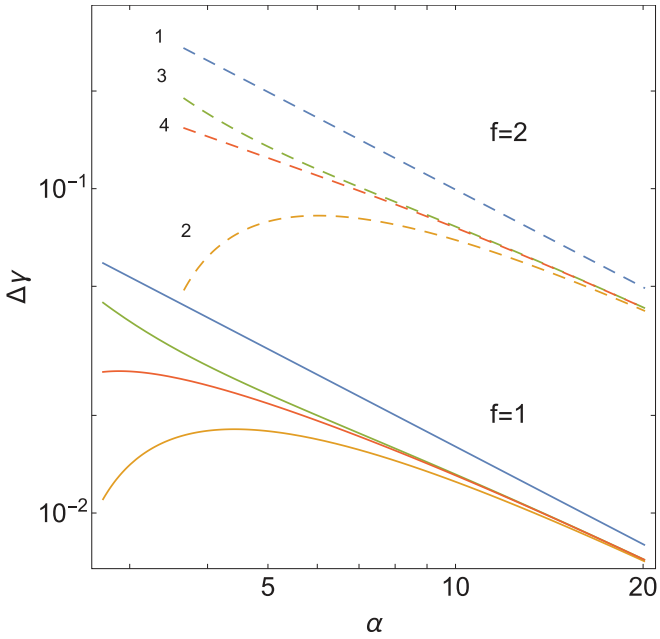

FIG. 3. Increment of the effective potential $\Delta\gamma$ over one period for Eq. (2.22), $f = 1$ (solid), and $f = 2$ (dashed lines). The numbers denote the highest order taken into account; the solid lines are ordered in the same way.

III. MAPPING BEYOND FJ APPROXIMATION

We include now the finite speed of the transverse relaxation across the channel in the mapping of Eq. (2.1). It is controlled by the auxiliary parameter ϵ, scaling the transverse diffusion constant to D_0/ϵ. We could continue looking for a better expression of $\rho_\pm(x, y, t)$ by $p_\pm(x, t)$, necessary in Eq. (2.3), taking a series of corrections to the FJ profile of $\rho_{\pm 0}$, Eq. (2.5), due to a nonzero ϵ. Having improved Eq. (2.6), we would reduce the orientation ($\pm$) as in Sec. II, expanding the deviations of $p_\pm(x, t)$ from $p(x, t)/2$ in $1/\alpha$.

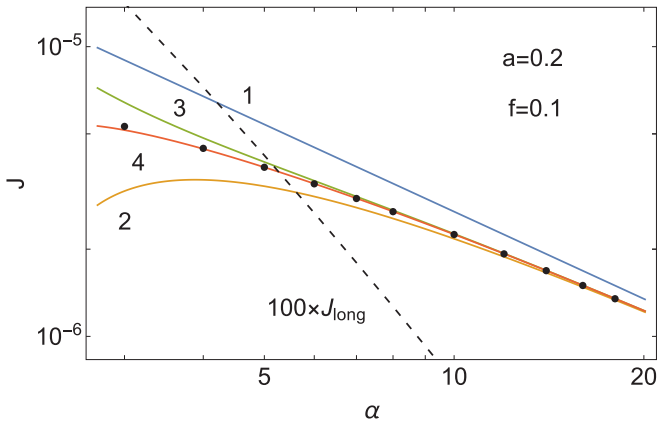

FIG. 4. The ratchet current J for the trial $h(x)$, Eq. (2.22), $f = 0.1$, taking $\gamma(x)$ and $1/D(x)$ truncated after the first, second, third, and fourth orders. The dots represent numerical solution of the 1D problem. The dashed line describes $100\times$ of the ratchet current driven in the same channel by the same force of longitudinal orientation.

Nevertheless, this strategy can be simplified by introducing $\bar{\alpha} = \epsilon\alpha$. If $\bar{\alpha}$ is hold finite, the flipping term in Eq. (2.1) becomes (formally) scaled in the same way as the transverse diffusion, $\sim 1/\epsilon$, like the next transverse coordinate. Then the limit $\epsilon \to 0$ equilibrates not only the profile in y, but also distribution of $(+)$ and $(-)$ particles.

The new equilibrated transverse profiles $\bar{\rho}_{\pm 0}$ are obtained by solving the equations

$$\partial_y(\partial_y \mp f)\bar{\rho}_{\pm 0}(x,y,t) \mp \bar{\alpha}(\bar{\rho}_{+0}(x,y,t) - \bar{\rho}_{-0}(x,y,t)) = 0, \tag{3.1}$$

given by the terms $\sim 1/\epsilon$ in Eq. (2.1), dominant in the FJ limit $\epsilon \to 0$. Defining the net 2D FJ density $\bar{\rho}_0(x,y,t) = \bar{\rho}_{+0}(x,y,t) + \bar{\rho}_{-0}(x,y,t)$ and the polarization density $\bar{\mu}_0(x,y,t) = \bar{\rho}_{+0}(x,y,t) - \bar{\rho}_{-0}(x,y,t)$, we need to solve the couple of differential equations in y:

$$\begin{aligned} \partial_y[\partial_y\bar{\rho}_0(x,y,t) - f\bar{\mu}_0(x,y,t)] &= 0, \\ \partial_y^2\bar{\mu}_0(x,y,t) - f\partial_y\bar{\rho}_0(x,y,t) - 2\bar{\alpha}\bar{\mu}_0(x,y,t) &= 0. \end{aligned} \tag{3.2}$$

The BCs (2.1) in the limit $\epsilon \to 0$ are reduced to

$$\begin{aligned} \partial_y\bar{\rho}_0(x,y,t) - f\bar{\mu}_0(x,y,t)|_{y=0,h(x)} &= 0, \\ \partial_y\bar{\mu}_0(x,y,t) - f\bar{\rho}_0(x,y,t)|_{y=0,h(x)} &= 0, \end{aligned} \tag{3.3}$$

at both boundaries. The new FJ approximation, represented by these equations, describes very fast relaxation in the transverse direction, as well as the orientation, but the ratio $\bar{\alpha}/D_0 = \bar{\alpha}$ comparing their rates is kept finite, which influences the solution. A trivial integration of the first Eq. (3.2) expresses the transverse flux of particles, which is zero due to the first BC (3.3). Substituting for $\partial_y\bar{\rho}_0$ in the second Eq. (3.2) and solving the system with BC (3.3), we get

$$\begin{aligned} \bar{\rho}_0 &= \left[1 + \frac{f^2[\sinh(qy) + \sinh(q[h(x)-y])]}{2\bar{\alpha}\sinh[qh(x)]}\right]R_0(x,t) \\ &= \hat{\eta}_0(x,y)R_0(x,y), \\ \bar{\mu}_0 &= \frac{fq[\cosh(qy) - \cosh(q[h(x)-y])]}{2\bar{\alpha}\sinh[qh(x)]}R_0(x,t) \\ &= \hat{\sigma}_0(x,y)R_0(x,y); \end{aligned} \tag{3.4}$$

we abbreviated $q = \sqrt{f^2 + 2\bar{\alpha}}$. The integration constant $R_0(x,t)$ (in y, appearing in the last integration of $\bar{\rho}_0$) can be related to the net 1D density $p(x,t)$, defined by Eqs. (2.4) and (2.7). Integrating $\bar{\rho}_0$, Eq. (3.4), over the cross section, we find

$$p(x,t) = \left[h(x) + \frac{f^2}{\bar{\alpha}q}\tanh\frac{qh(x)}{2}\right]R_0(x,t). \tag{3.5}$$

The relations (3.4) together with the normalization (3.5) represent the zeroth order formulas, mapping the 1D density $p(x,t)$ backward onto the space of 2D densities $\rho_\pm(x,y,t) = (\bar{\rho}_0(x,y,t) \pm \bar{\mu}_0(x,y,t)/2$. If applied in Eqs. (2.3) summed over both orientations, we arrive at

$$\partial_t p(x,t) = \partial_x\left[\partial_x - \frac{q^3h'(x)}{2(\bar{\alpha}qh(x) + f^2\tanh[qh(x)/2])}\right]p(x,t), \tag{3.6}$$

the new FJ equation. It can also be written in the form of $\partial_t p = \partial_x\tilde{A}_0\partial_x(p/\tilde{A}_0)$, where the function

$$\tilde{A}_0(x) = \exp\left[\int \frac{q^3\,dh(x)}{2(\bar{\alpha}qh(x) + f^2\tanh[qh(x)/2])}\right] \tag{3.7}$$

up to an irrelevant integration constant. Here $\tilde{A}_0(x)$ cannot be expressed by an explicit formula for an arbitrary $h(x)$, but it is evident that it is a function of $h(x)$. So, it cannot exhibit an increment over period L for any periodic function $h(x) = h(x+L)$; i.e., it gives no contribution to the effective potential driving the ratchet.

Nevertheless, the new FJ (zeroth order) Eq. (3.6) involves a series of new terms with respect to the former FJ, Eqs. (2.9) and (2.10). If we return $\bar{\alpha} = \epsilon\alpha$ in the formula (3.7) and expand it in ϵ, the zeroth order recovers Eq. (2.10) (having properly set the integration constant). To handle with $\tilde{A}_0(x)$ conveniently in our next calculations, we rewrite it using

$$\begin{aligned} \bar{A}_0(x) &= e^{-\bar{\gamma}_0(x)}\tilde{A}_0(x) = h(x) + \frac{f^2}{\bar{\alpha}q}\tanh\frac{qh(x)}{2}, \\ \bar{\gamma}_0'(x) &= \frac{f^2h'(x)}{2\bar{\alpha}\bar{A}_0(x)}\tanh^2\frac{qh(x)}{2}, \end{aligned} \tag{3.8}$$

reflecting the normalization relation (3.5).

The corrections to Eq. (3.6) due to slower relaxation in the fast transverse coordinates can be derived after extending the backward mapping relations (3.4) by the series of correction terms in ϵ, controlling the speed of relaxation. Consistently with similar calculations [36,41], the 2D densities $\rho_\pm(x,y,t) = [\rho(x,y,t) \pm \mu(x,y,t)]/2$ are expected in the form

$$\begin{aligned} \rho(x,y,t) &= e^{\bar{\gamma}(x)}\hat{\eta}(x,y,\partial_x)\frac{p(x,t)}{\bar{A}(x)}, \\ \mu(x,y,t) &= e^{\bar{\gamma}(x)}\hat{\sigma}(x,y,\partial_x)\frac{p(x,t)}{\bar{A}(x)}; \\ \bar{A}(x) &= \bar{A}_0(x)e^{\bar{\gamma}(x)}. \end{aligned} \tag{3.9}$$

The operators $\hat{\eta}$, $\hat{\sigma}$, the gauge function $\bar{\gamma}(x)$, as well as the related quantities which will be introduced later, are expanded in ϵ,

$$F(.) = \sum_{n=0}^{\infty}\epsilon^n F_n(.). \tag{3.10}$$

The zeroth order terms $\hat{\eta}_0$, $\hat{\sigma}_0$, and $\bar{\gamma}_0$ are already fixed; Eqs. (3.9) have to resume the FJ relations (3.4), (3.5), and (3.8) for $\epsilon = 0$. The next orders will be derived recursively. Unlike the zeroth order terms, the higher order $\hat{\eta}_n$ and $\hat{\sigma}_n$ also have parts containing the derivatives ∂_x; they can be split to $\hat{\eta}_n(x,y,\partial_x) = \tilde{\eta}_n(x,y,\partial_x)\partial_x + \eta_n(x,y)$ and $\hat{\sigma}_n(x,y,\partial_x) = \tilde{\sigma}_n(x,y,\partial_x)\partial_x + \sigma_n(x,y)$, where η_n and σ_n denote just functions. If the relations (3.9) are substituted in Eqs. (2.3) summed over the orientation, the obtained mapped equation

$$\begin{aligned} \partial_t p(x,t) = \partial_x\bar{A}(x)\Bigg(&\partial_x + \bar{\gamma}'(x) + \frac{\bar{A}_0'(x)}{\bar{A}_0(x)} \\ &- \frac{h'(x)}{\bar{A}_0(x)}\hat{\eta}[x,h(x),\partial_x]\Bigg)\frac{p(x,t)}{\bar{A}(x)} \end{aligned} \tag{3.11}$$

can be transformed to the form (1.1) by the proper setting of $\bar\gamma(x)$. It has to clear all the contributions not containing ∂_x in the big brackets of Eq. (3.11); the rest gives the corrections to the operator $\hat Z(x,\partial_x)$. Having used $\hat\eta_0=\eta_0$ according to Eqs. (3.4) and $\bar A_0(x)$ in the zeroth order of Eq. (3.11), we can easily verify the formula (3.8) fixing $\bar\gamma_0'$. For the higher orders, we have

$$\bar\gamma_n'(x)=\frac{h'(x)}{\bar A_0(x)}\eta_n[x,h(x)],$$
$$\hat Z_n(x,\partial_x)=\frac{h'(x)}{\bar A_0(x)}\tilde\eta_n[x,h(x),\partial_x]. \tag{3.12}$$

To fix the operators $\hat\eta_n$, $\hat\sigma_n$, we require that the original 2D problem was satisfied by the $\rho_\pm(x,y,t)$ obtained by the relations (3.9) of backward mapping for any 1D solution $p(x,t)$. Substituting them in Eqs. (2.1), we get

$$\begin{aligned}\partial_t e^{\bar\gamma}\hat\eta\frac{p}{A}&=\partial_x^2 e^{\bar\gamma}\hat\eta\frac{p}{A}+\frac{1}{\epsilon}\partial_y\Big(\partial_y e^{\bar\gamma}\hat\eta\frac{p}{A}-fe^{\bar\gamma}\hat\sigma\frac{p}{A}\Big),\\ \partial_t e^{\bar\gamma}\hat\sigma\frac{p}{A}&=\partial_x^2 e^{\bar\gamma}\hat\sigma\frac{p}{A}+\frac{1}{\epsilon}\Big[\partial_y\Big(\partial_y e^{\bar\gamma}\hat\sigma\frac{p}{A}-fe^{\bar\gamma}\hat\eta\frac{p}{A}\Big)\\ &\quad-2\bar\alpha e^{\bar\gamma}\hat\sigma\frac{p}{A}\Big]\end{aligned} \tag{3.13}$$

after their summation and subtraction, respectively; we omit writing the arguments since now. The time derivative ∂_t commutes here with all spatial operators to the right and $\partial_t p(x,t)$ is replaced by the right-hand side of Eqs. (1.1). Expressing the terms $\sim 1/\epsilon$ from the equations, we find

$$\begin{aligned}\frac{1}{\epsilon}\partial_y(\partial_y\hat\eta-f\hat\sigma)&=\hat\eta\frac{1}{A}\partial_x A(1-\hat Z)\partial_x-e^{-\bar\gamma}\partial_x^2e^{\bar\gamma}\hat\eta,\\ \frac{1}{\epsilon}[\partial_y(\partial_y\hat\sigma-f\hat\eta)-2\bar\alpha\hat\sigma]&=\hat\sigma\frac{1}{A}\partial_x A(1-\hat Z)\partial_x\\ &\quad-e^{-\bar\gamma}\partial_x^2e^{\bar\gamma}\hat\sigma,\end{aligned} \tag{3.14}$$

acting on an arbitrary function $p(x,t)/A(x)$. Expanding all the operators and functions in these equations in ϵ and collecting the terms of the same orders, we get the recurrence scheme of the form

$$\begin{aligned}\partial_y(\partial_y\hat\eta_n-f\hat\sigma_n)&=\hat R_n(x,y,\partial_x),\\ \partial_y(\partial_y\hat\sigma_n-f\hat\eta_n)-2\bar\alpha\hat\sigma_n&=\hat T_n(x,y,\partial_x);\end{aligned} \tag{3.15}$$

the operators $\hat R_n(x,y,\partial_x)$ and $\hat T_n(x,y,\partial_x)$ are composed of the lower-order coefficients of $\hat\eta$, $\hat\sigma$, $\hat Z$, and γ. The solutions have to satisfy the BCs

$$\begin{aligned}(\partial_y\hat\eta-f\hat\sigma)|_{y=0}&=0,\\ (\partial_y\hat\eta-f\hat\sigma)|_{y=h(x)}&=\epsilon h'e^{-\bar\gamma}\partial_x e^{\bar\gamma}\hat\eta|_{y=h(x)},\\ (\partial_y\hat\sigma-f\hat\eta)|_{y=0}&=0,\\ (\partial_y\hat\sigma-f\hat\eta)|_{y=h(x)}&=\epsilon h'e^{-\bar\gamma}\partial_x e^{\bar\gamma}\hat\sigma|_{y=h(x)}\end{aligned} \tag{3.16}$$

in particular orders of ϵ^n, coming from Eqs. (2.2) with use of the relations (3.9). Finally, the backward mapped $\rho(x,y,t)$ applied in the definitions (2.3) and (2.7) has to give an identity, hence

$$\int_0^{h(x)}\hat\eta_n(x,y,\partial_x)dy=0 \tag{3.17}$$

for $n>0$.

The terms $\sim\epsilon^{-1}$ in Eqs. (3.14) give Eqs. (3.2), determining $\hat\eta_0$ and $\hat\sigma_0$, Eqs. (3.4). In the higher orders, the trivial integration of the first Eq. (3.15),

$$\partial_y\hat\eta_n-f\hat\sigma_n=\int_0^y\hat R_n(x,y',\partial_x)dy'=\hat Q_n(x,y,\partial_x),$$

satisfies the first two BCs (3.16). If it is substituted in the second Eq. (3.15), it is solved by

$$\begin{aligned}\hat\sigma_n&=\Big(\int\frac{\cosh qy}{q}[\hat T_n+f\hat Q_n]dy+\hat S_n\Big)\sinh(qy)\\ &\quad-\Big(\int\frac{\sinh qy}{q}[\hat T_n+f\hat Q_n]dy+\hat C_n\Big)\cosh(qy);\end{aligned} \tag{3.18}$$

the integration constants $\hat S_n(x,\partial_x)$, $\hat C_n(x,\partial_x)$ are fixed to satisfy the last two BCs (3.16). Finally, the integration constant $\hat K_n(x,\partial_x)$ in the last integral,

$$\hat\eta_n=\int[\hat Q_n+f\hat\sigma_n]dy+\hat K_n(x,\partial_x), \tag{3.19}$$

is determined from the normalization condition (3.17). Having finally derived the operator $\hat\eta_n(x,y,\partial_x)$, we fix $\bar\gamma_n'(x)$ and $\hat Z_n(x,\partial_x)$ according to Eqs. (3.12). Notice that we do not need to integrate $\bar\gamma_n'$ explicitly within the recurrence scheme.

The leading corrections $\hat\eta_1$, $\hat\sigma_1$ to the FJ are obtained by collecting the terms $\sim\epsilon^0$ in Eqs. (3.14):

$$\begin{aligned}\hat R_1&=\hat\eta_0\Big(\partial_x+\frac{\bar A_0'}{\bar A_0}+\bar\gamma_0'\Big)\partial_x-(\partial_x+\bar\gamma_0')^2\hat\eta_0\\ &=\Big[\hat\eta_0\Big(\frac{\bar A_0'}{\bar A_0}-\bar\gamma_0'\Big)-2\hat\eta_0'\Big]\partial_x-\hat\eta_0\big(\bar\gamma_0''+\hat\gamma_0'^2\big)-\hat\eta_0'',\\ \hat T_1&=\Big[\hat\sigma_0\Big(\frac{\bar A_0'}{\bar A_0}-\bar\gamma_0'\Big)-2\hat\sigma_0'\Big]\partial_x-\hat\sigma_0\big(\bar\gamma_0''+\hat\gamma_0'^2\big)-\hat\sigma_0''.\end{aligned} \tag{3.20}$$

As $\hat\eta_0$ and $\hat\sigma_0$, Eqs. (3.4), are just functions, and the solution of the corresponding Eqs. (3.15) deals with only the y coordinate; the resultant $\hat\eta_1$ and $\hat\sigma_1$ will also consist of the parts $\sim\partial_x$ and just functions. Despite a simple scheme (3.18)–(3.19), the calculation is tedious and the result is rather complicated even in the first order. We state here only the final coefficients

$$\begin{aligned}\bar\gamma_1'=&\frac{-f^2h'}{24\bar\alpha\cosh^3\kappa}[qh'^2\sinh\kappa+h''(2\cosh\kappa+\cosh3\kappa)]-\frac{f^2h'}{96\bar\alpha^2q\bar A_0\cosh^4\kappa}[qh'^2(14\bar\alpha+19f^2+[6\bar\alpha-8f^2]\\ &\times\cosh2\kappa+[4\bar\alpha+f^2]\cosh4\kappa)+6h''(\bar\alpha+2f^2)\sinh2\kappa]\\ &+\frac{f^2h'\tanh\kappa}{32\bar\alpha^3q^2\bar A_0^2\cosh^4\kappa}[qh'^2(3\bar\alpha^2+8\bar\alpha f^2+15f^4+[4\bar\alpha^2-4\bar\alpha f^2-5f^4]\cosh2\kappa+\bar\alpha^2\cosh4\kappa)\end{aligned}$$

$$+h''(2\bar{\alpha}^2+6\bar{\alpha}f^2+[2\bar{\alpha}^2+2\bar{\alpha}f^2+f^4]\cosh 2\kappa)\sinh 2\kappa]$$
$$+\frac{f^4h'\tanh^2\kappa}{384\bar{\alpha}^4q^3\bar{A}_0^3\cosh^4\kappa}[qh'^2(60\bar{\alpha}^2-18\bar{\alpha}f^2-179f^4+4[15\bar{\alpha}^2-9\bar{\alpha}f^2+8f^4]\cosh 2\kappa+3[4\bar{\alpha}^2+2\bar{\alpha}f^2+f^4]$$
$$\times\cosh 4\kappa)+8h''(3\bar{\alpha}^2-6\bar{\alpha}f^2-5f^4+[3\bar{\alpha}^2-3\bar{\alpha}f^2-f^4]\cosh 2\kappa)\sinh 2\kappa]$$
$$-\frac{f^4h'^3\tanh^3\kappa}{192\bar{\alpha}^5q^3\bar{A}_0^4\cosh^4\kappa}[18\bar{\alpha}^3-15\bar{\alpha}^2f^2-55\bar{\alpha}f^4-29f^6+(24\bar{\alpha}^3-24\bar{\alpha}^2f^2-30\bar{\alpha}f^4+4f^6)\cosh 2\kappa$$
$$+(6\bar{\alpha}^3-9\bar{\alpha}^2f^2+\bar{\alpha}f^4+f^6]\cosh 4\kappa],$$
$$\hat{Z}_1=h'^2\left\{\frac{1}{3}-\frac{f^2\cosh 2\kappa}{12\bar{\alpha}\cosh^2\kappa}-\frac{f^2(\bar{\alpha}+2f^2)\tanh\kappa}{4\bar{\alpha}^2q\bar{A}_0\cosh^2\kappa}-\frac{f^2}{8\bar{\alpha}^3q^2\bar{A}_0^2}\left[\frac{(2\bar{\alpha}+3f^2)}{\cosh^2\kappa}\left(\bar{\alpha}+f^2\frac{(1-\sinh^2\kappa)}{\cosh^2\kappa}\right)-4\bar{\alpha}^2-2\bar{\alpha}f^2-f^4\right]\right.$$
$$-\frac{f^2\tanh\kappa}{96\bar{\alpha}^4q^3\bar{A}_0^3\cosh^4\kappa}[18\bar{\alpha}^3-15\bar{\alpha}^2f^2-55\bar{\alpha}f^4-29f^6+2(12\bar{\alpha}^3-12\bar{\alpha}^2f^2-15\bar{\alpha}f^4+2f^6)\cosh 2\kappa$$
$$\left.+(6\bar{\alpha}^3-9\bar{\alpha}^2f^2+\bar{\alpha}f^4+f^6)\cosh 4\kappa)]\right\}, \tag{3.21}$$

entering the generalized FJ Eqs. (1.1); $\kappa = qh(x)/2$. The leading correction $\hat{Z}_1$ is just a function, so according to Eq. (2.19), $D(x) = 1 - \epsilon\hat{Z}_1(x)$ up to first order. Of course, ϵ is also hidden in $\bar{\alpha} = \epsilon\alpha$, if we return back to the original formulation, Eq. (2.1), where the flipping rate α is fixed. Thus the formulas (3.21) represent again series of terms, correcting $\bar{A}_0$ and $D(x)$ due to the flipping and finite transverse relaxation rate. We can immediately discern Zwanzig's leading correction $h'^2/3$ in $\hat{Z}_1$. The other terms are proportional at least to f^2, representing the corrections due to driving, extending Zwanzig's factor 1/3. If α is fixed, the term with tanh in $\bar{A}_0$, Eqs. (3.8), becomes dominant, diverging as $1/\epsilon$ in the limit $\epsilon \to 0$. The function $\bar{\gamma}_0'$, Eqs. (3.8), becomes integrable explicitly and $\bar{A}_0 e^{\bar{\gamma}_0} \to A_0$, Eq. (2.10), up to an irrelevant constant factor. Also, the formulas for $\epsilon\bar{\gamma}_1'$ and $\epsilon\hat{Z}_1$ approach $\gamma_1'/(2\alpha)$, and $\hat{Z}_1/(2\alpha)$ according to Eqs. (2.17). Extending the presented recurrence procedure to the higher orders is technically demanding, so to study the basic influence of the finite transverse relaxation to the ratchet effect, we only replace the lowest order terms of $\gamma'(x)$ and $1/D(x)$ from Sec. II by Eqs. (3.8) and (3.21). Figure 5(a) shows $D(x)$ with the leading correction $\hat{Z}_1$, Eqs. (3.21) (solid line), compared with Zwanzig's term (dashed line), for the channel shaped by Eq. (2.22), $a = 0.2$. Even for values $f = 1$ and $\alpha = 5$, at the border of usability of the truncated expansion, the corrections due to stochastic driving only slightly increase $D(x)$ in the style of Taylor dispersion. Still, behavior of $D(x)$ is determined mainly by retarding of the transverse diffusion due to corrugation, as described by Zwanzig [33] or Reguera-Rubí's (RR) [34] formula if all the terms depending only on h' are summed [32]. In the first order, Zwanzig's factor 1/3 standing at h'^2 is corrected, see Fig. 5(b). It is decreased roughly by $f^2/(6\bar{\alpha})$, given by the second term of $\hat{Z}_1$ in Eqs. (3.21) for $\kappa \to \infty$.

The complicated formula for $\bar{\gamma}_1'$ results again in additional potential $-\gamma(x)$ after integration, giving a nonzero increment $\Delta\gamma$ over one period $L = 2\pi$ for asymmetric channels. Figure 6 demonstrates dependence of $\Delta\gamma$ on the flipping rate α for our trial channel, Eq. (2.22); $a = 0.2$, $f = 0.5$, and various ϵ from 0 to 1 (solid lines). The line for $\epsilon = 0$ is identical to $\Delta\gamma$ from the Sec. II obtained for $\gamma(x)$ up to fourth order. For $\epsilon > 0$, we replaced the term $\gamma_1(x)/(2\alpha)$ by $\epsilon\bar{\gamma}_1(x)$, Eqs. (3.21). Figure 5 shows that unlike the longitudinal driving [36], con-

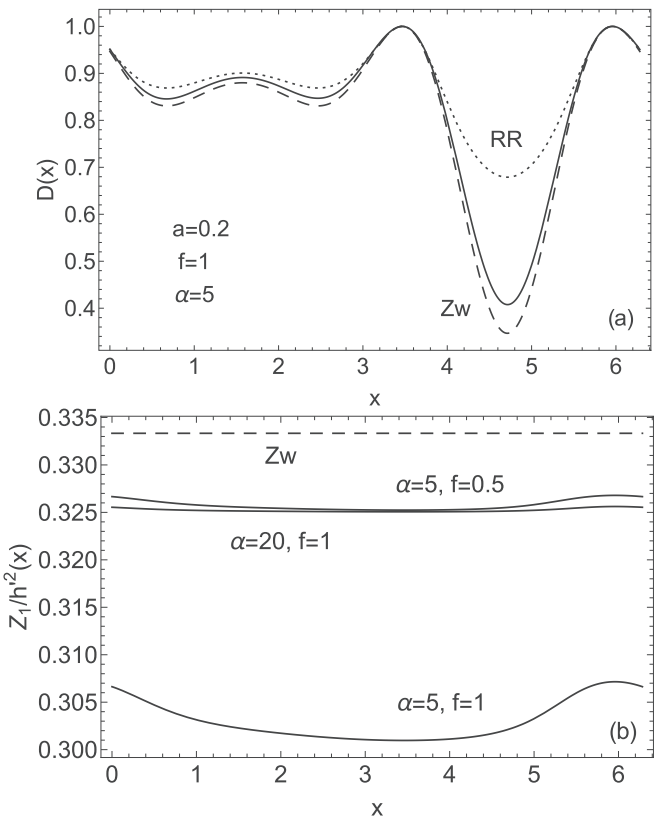

FIG. 5. (a) The effective diffusion coefficient $D(x)$ for the trial function $h(x)$, Eq. (2.22) according to $\hat{Z}_1$, Eqs. (3.21), $\epsilon = 1$, $f = 1$ and $\alpha = 5$ (solid line). It is compared with Zwanzig's correction, $1 - h'^2/3$ (Zw, dashed) and the Reguera-Rubí formula $D(x) = (1 + h'^2)^{-1/3}$, (RR, dotted line). b) Coefficient at h'^2 in $\hat{Z}_1$ for several values of f and α, compared with Zwanzig's value 1/3 (Zw, dashed line).

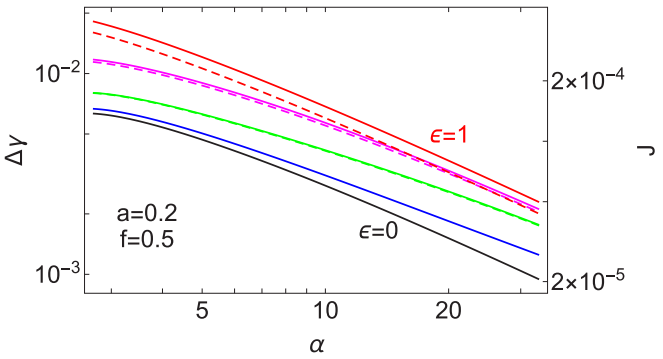

FIG. 6. Increment of the effective potential $\Delta\gamma$ according to Eqs. (3.21) over one period (solid lines, left scale) and the corresponding rectified current J (dashed, right scale) in the channel defined by Eq. (2.22), $a = 0.2$, depending on the flipping rate α of the force $f = 0.5$. The lines for various ϵ are ranged from $\epsilon = 0$ (black), 0.01 (blue), 0.05 (green), 0.2 (magenta), to 1 (red).

sidering a finite transverse relaxation rate in the leading term does not change dramatically behavior of the dependence, i.e., the values obtained by the FJ approximation (Sec. II) are only slightly increased with growing ϵ. The ratchet current J is determined almost thoroughly by $\Delta\gamma$, multiplied by some factor (∼mobility) depending on ϵ and mainly geometry of the channel. The dashed lines in Fig. 6 plot J (scaled on the right axis) of parameters corresponding to $\Delta\gamma$ of the same color; for smaller $\epsilon < 0.1$, the dashed and solid lines cannot be discerned.

The backward mapping relations (3.9) enable us to reconstruct the 2D picture corresponding to any solution $p(x,t)/A(x)$ of the reduced 1D problem, Eq. (1.2). For the stationary flow with one particle per period, we obtain the 2D density $\rho(x,y)$ (color scale) and the current density (streamlines) as described in Figs. 7; see the Appendix for details. The fluctuating force spins a couple of counter-directional whirls in a compartment of the channel. They are not symmetric because of asymmetry of the channel. The resulting net flux J leaks between them, securing periodicity of the solution. The particles are pushed to the top of the bulges, then, after flipping the force, they form the second maximum of the density at the bottom flat side of the channel. The minimum density is observed near the centerline, depicted by the dotted line. If we compare Figs. 7(a) and 7(b), calculated for $\epsilon = 0.02$ and 0.1, respectively, the slower transverse diffusion smears the difference betweenthe maximum and minimum of the density; as probability of the next flip of the force during the slower movement to the opposite side grows. Still, as the transverse flux $\sim 1/\epsilon$, we obtain in combination with smaller gradients of the density a similar pattern of streamlines (current density), also giving the net flux without marked changes.

Although ϵ was introduced as an auxiliary parameter to separate the fast transverse relaxation from the slower longitudinal processes, also the values $\epsilon < 1$ are meaningful. Scaling of the transverse diffusion constant is equivalent to shrinking the transverse lengths by $\sqrt{\epsilon}$ and, correspondingly, the force f by $1/\sqrt{\epsilon}$. Thus, the results for smaller ϵ describe the transport in thinner channels with stronger driving, but isotropic diffusion constant D_0.

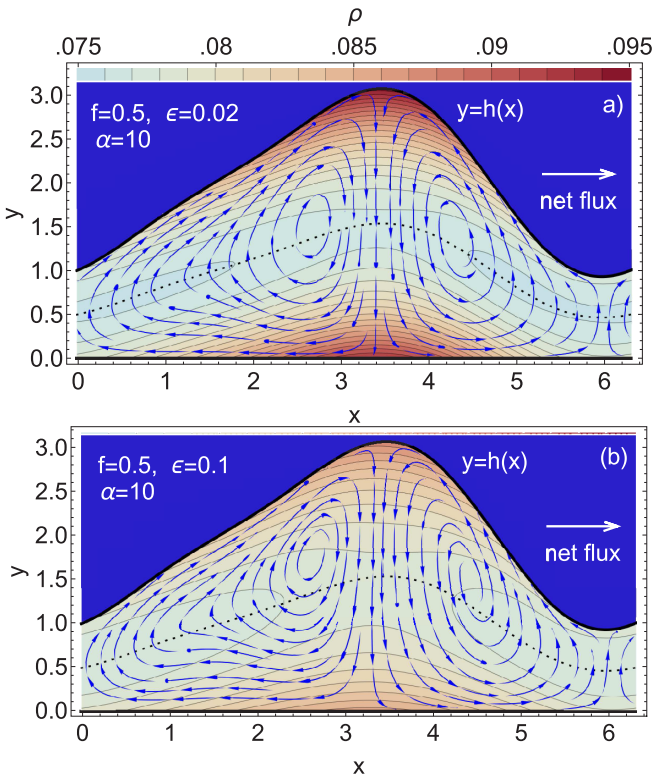

FIG. 7. Stationary 2D density $\rho(x,y)$ (color scale) and the fluxes (streamlines) in the channel with $a = 0.2$ for $\epsilon = 0.02$ (a) and 0.1 (b). The dotted line depicts the centerline. The rectified current flows to the right with magnitudes $J = 1.16 \times 10^{-4}$ (a) and 8.5×10^{-5} (b) for one particle per period $L = 2\pi$.

IV. CONCLUSION

The models of diffusing particles confined in a nonhomogeneous channel and driven by stochastic forces are often used to study the systems of active particles. In an effective 1D picture, the force is usually considered to flip only in the longitudinal direction. To extend the effective description to real 2D systems, one also needs to consider flipping in the directions which are reduced by the mapping. So we studied here a similar model of a confined diffusing particle in which the driving force flips across the channel.

Primarily, our aim was to extend the mapping technique for various orientations of the flipping force. Similar to the longitudinal driving [30,36], mapping of diffusion driven by the transverse force also leads to an effective 1D equation of the generalized FJ form. Its zeroth order is based on an infinitely fast relaxation to a specific nonuniform transverse distribution, determined by the transverse force and its flipping [Eqs. (2.5) or (3.4)]. Finite speed of the transverse relaxation, as well as the persistence time $\sim 1/\alpha > 0$ requires us to include corrections, represented by the operator $\hat{Z}$ or the spatial-dependent effective diffusion coefficient $D(x)$ and the function $\gamma(x)$ in Eqs. (1.1) and (1.2). They are found as a series in an auxiliary parameter ϵ, scaling the transverse diffusion constant and the flipping rate α. The limit $\epsilon \to 0$ describes immediate transverse relaxation, giving the basic FJ

equation. Otherwise, ϵ controls the expansion of $\hat{Z}$ and $\gamma(x)$, whose coefficients are derived recursively. The parameter $\epsilon \neq 1$ can also be interpreted as describing the channel $\sqrt{\epsilon}$-times thinner and the force $f/\sqrt{\epsilon}$ with an isotropic diffusion constant D_0.

Our interest is then focused on the ratchet effect, which can appear in such systems. The function $-\gamma(x)$ represents an additional effective potential, extending the obvious entropic potential, appearing here due to the flipping force. It becomes a slanted washboard function in periodic asymmetric channels, exhibiting a nonzero increment $\Delta\gamma$ over one period. The slope represents the effective force, giving rise to the ratchet current J, proportional roughly to $\Delta\gamma$.

It is interesting to compare the results for the complementary models with the longitudinal [36] and the presented transverse driving by the force of the same magnitude in the same channel. The changed orientation of the flipping force results in a markedly different behavior of the ratchet current. The asymptotic of $\Delta\gamma \sim 1/\alpha$ in the limit of large α in the case of transverse driving, while it decreases much faster $\sim 1/\alpha^3$, if driven in the longitudinal direction, especially for small ϵ. Thus the transverse driving appears to be more effective than the longitudinal one, Fig. 4, at least for large α. The engine spinning the couples of asymmetric whirls, visible in Fig. 7, and moving the net current, works at the curved boundary, where the equilibrium between (+) and (−) particles is violated because of different BCs. Unlike the transverse driving, the longitudinal flipping force can move a part of the particles without touching the curved boundary. Finally, comparing Figs. 7 in Ref. [36] and the present paper, the asymmetric whirls in a compartment of the channel rotate in opposite directions for the longitudinal versus transverse driving and also the ratchet currents flow in opposite directions in the particular cases. Reverting the current direction caused by changing the orientation of the flipping force may recall the current reversal in the rocking ratchets driven by the oscillating force in higher frequencies [42–44], but the origin of this effect is different; there is no phase shift between the oscillating density and the force here.

The expansions of $D(x)$ and $\gamma(x)$ used here are controlled by inverse of α, either directly or using the scaling by ϵ, so they work well only for larger α [>5 for our trial shaping function (2.22)]. Knowing the structure of the mapping, one can formulate an alternative theory, as done for the simplest 1D model with longitudinal driving [30], finding directly the differential equations for $\gamma(x)$ and $D(x)$ without restrictions on α or f. On the other hand, also the simplest formulas, like Eqs. (2.17), (2.18), or (3.21), determining the asymptotic behavior of the ratchet are meaningful. Calculation of the leading term of the increment $\Delta\gamma$ over one period can estimate very effectively the direction and magnitude of the ratchet current, which is not a trivial task using either the numerical simulations or some qualitative analysis.

ACKNOWLEDGMENTS

Support from VEGA Grant No. 2/0044/21 is gratefully acknowledged.

APPENDIX: COMPUTATIONAL DETAILS

Here we give details of several calculations in the text. Equation (2.19) relating the effective diffusion coefficient $D(x)$ and the operator $\hat{Z}$ is found using two different formulas for the net flux $J(x,t)$ flowing in the channel:

$$J(x,t) = -D_0 A(x)[1-\hat{Z}(x,\partial_x)]\partial_x \frac{p(x,t)}{A(x)},$$
$$J(x,t) = -A(x)D(x)\partial_x \frac{p(x,t)}{A(x)}. \tag{A1}$$

They come from Eqs. (1.1) and (1.2), respectively, as both represent the 1D mass conservation, $\partial_x p = -\partial_x J$. In the stationary limit, p becomes independent of time, hence the net flux $J(x,t) = J$ is constant. The derivative $\partial_x(p/A)$ has to be the same for a given J and all parameters of the system, if expressed from either of the equations. Comparing both formulas for $\partial_x(p/A)$, one arrives at Eq. (2.19).

The simpler form of Eqs. (A1) enables us to write the 1D stationary solution $p_s(x)$ as

$$\frac{p_s(x)}{A(x)} = \rho_0 - \int_0^x \frac{J\,dx'}{A(x')D(x')}. \tag{A2}$$

In a periodic channel, $h(x+L) = h(x)$, we set the integration constant ρ_0 to fix one particle per period L. To describe the stationary flow, we require periodicity of the 1D density $p_s(x) = p_s(x+L)$. If $\gamma(x+L) - \gamma(x) = \Delta\gamma$ is nonzero, $A(x)$ [unlike $A_0(x)$ and $D(x)$] is not periodic:

$$A(x+L) = A_0(x+L)e^{\gamma(x+L)} = A(x)e^{\Delta\gamma}. \tag{A3}$$

Applying (A3) in the condition of periodicity, we find

$$(1-e^{-\Delta\gamma})\rho_0 = \int_0^L \frac{J\,dx'}{A(x')D(x')},$$

hence after using Eq. (A3) and some algebra:

$$\frac{p_s(x)}{A(x)} = \frac{J}{(e^{\Delta\gamma}-1)} \int_{x-L}^{L} \frac{dx'}{A(x')D(x')}. \tag{A4}$$

Normalizing $\int_0^L p_s(x)dx = 1$, we obtain Eq. (2.21).

Knowing the stationary 1D density $p_s(x)$, we can reconstruct the corresponding 2D densities by the backward mapping, Eqs. (3.9). The net 2D stationary density

$$\rho_s(x,y) = e^{\bar{\gamma}(x)}\hat{\eta}(x,y,\partial_x)\frac{p_s(x)}{\bar{A}(x)} \tag{A5}$$

is depicted in Fig. 7 by colors; $\bar{A}(x)$ replaces $A(x)$ in Eq. (A4). The streamlines are calculated according to the components of the stationary net current density:

$$j_x(x,y) = -\partial_x e^{\bar{\gamma}(x)}\hat{\eta}(x,y,\partial_x)\frac{p_s(x)}{\bar{A}(x)},$$
$$j_y(x,y) = \frac{1}{\epsilon}e^{\bar{\gamma}(x)}[f\hat{\sigma}(x,y,\partial_x) - \partial_y\hat{\eta}(x,y,\partial_x)]\frac{p_s(x)}{\bar{A}(x)}. \tag{A6}$$

[1] P. Reimann, Phys. Rep. **361**, 57 (2002).
[2] P. Hänggi and F. Marchesoni, Rev. Mod. Phys. **81**, 387 (2009).
[3] A. Ryabov, V. Holubec, M. H. Yaghoubi, M. Varga, A. Khodaee, M. E. Foulaadvand, and P. Chvosta, J. Stat. Mech.: Theory Exp. (2016) 093202.
[4] V. Holubec, A. Ryabov, M. H. Yaghoubi, M. Varga, A. Khodaee, M. E. Foulaadvand, and P. Chvosta, Entropy **19**, 119 (2017).
[5] P. Kalinay and F. Slanina, Phys. Rev. E **98**, 042141 (2018).
[6] M. H. Jacobs, *Diffusion Processes* (Springer, New York, 1967).
[7] P. Romanczuk, M. Bär, W. Ebeling, B. Lindner, and L. Schimansky-Geier, Eur. Phys. J.: Spec. Top. **202**, 1 (2012).
[8] E. Fodor and M. C. Marchetti, Physica A **504**, 106 (2018).
[9] P. Galajda, J. Keymer, P. Chaikin, and R. Austin, J. Bacteriol. **189**, 8704 (2007).
[10] L. F. Valadares, Y.-G. Tao, N. S. Zacharia, V. Kitaev, F. Galembeck, R. Kapral, and G. A. Ozin, Small **6**, 565 (2010).
[11] A. Walther and A. H. E. Müller, Chem. Rev. **113**, 5194 (2013).
[12] A. Sokolov, M. M. Apodaca, B. A. Grzybowski, and I. S. Aranson, Proc. Natl. Acad. Sci. USA **107**, 969 (2010).
[13] R. Di Leonardo, L. Angelani, D. Dell'Arciprete, G. Ruocco, V. Iebba, S. Schippa, M. P. Conte, F. Mecarini, F. De Angelis, and E. Di Fabrizio, Proc. Natl. Acad. Sci. USA **107**, 9541 (2010).
[14] G. Volpe, I. I. Buttinoni, D. Vogt, H.-J. Kümmerer, and C. Bechinger, Soft Matter **7**, 8810 (2011).
[15] M. B. Wan, C. J. Olson Reichhardt, Z. Nussinov, and C. Reichhardt, Phys. Rev. Lett. **101**, 018102 (2008).
[16] I. Berdakin, Y. Jeyaram, V. V. Moshchalkov, L. Venken, S. Dierckx, S. J. Vanderleyden, A. V. Silhanek, C. A. Condat, and V. I. Marconi, Phys. Rev. E **87**, 052702 (2013).
[17] C. J. Olson Reichhardt and C. Reichhardt, Annu. Rev. Condens. Matter Phys. **8**, 51 (2017).
[18] P. K. Ghosh, V. R. Misko, F. Marchesoni, and F. Nori, Phys. Rev. Lett. **110**, 268301 (2013).
[19] P. K. Ghosh, P. Hänggi, F. Marchesoni, and F. Nori, Phys. Rev. E **89**, 062115 (2014).
[20] B.-Q. Ai, Y.-F. He, and W.-R. Zhong, J. Chem. Phys. **141**, 194111 (2014).
[21] K. Bisht and R. Marathe, Phys. Rev. E **101**, 042409 (2020).
[22] L. Angelani, A. Costanzo, and R. Di Leonardo, Europhys. Lett. **96**, 68002 (2011).
[23] N. Koumakis, C. Maggi, and R. Di Leonardo, Soft Matter **10**, 5695 (2014).
[24] A. Pototsky, A. M. Hahn, and H. Stark, Phys. Rev. E **87**, 042124 (2013).
[25] M. Sandoval and L. Dagdug, Phys. Rev. E **90**, 062711 (2014)
[26] E. Yariv and O. Schnitzer, Phys. Rev. E **90**, 032115 (2014).
[27] P. Malgaretti and H. Stark, J. Chem. Phys. **146**, 174901 (2017).
[28] M. Kahlen, A. Engel, and Ch. Van den Broeck, Phys. Rev. E **95**, 012144 (2017).
[29] E. Aurell and S. Bo, Phys. Rev. E **96**, 032140 (2017).
[30] P. Kalinay, Phys. Rev. E **104**, 014608 (2021).
[31] P. Kalinay and J. K. Percus, J. Chem. Phys. **122**, 204701 (2005).
[32] P. Kalinay and J. K. Percus, Phys. Rev. E **74**, 041203 (2006).
[33] R. Zwanzig, J. Phys. Chem. **96**, 3926 (1992).
[34] D. Reguera and J. M. Rubí, Phys. Rev. E **64**, 061106 (2001).
[35] S. Martens, G. Schmid, L. Schimansky-Geier, and P. Hänggi, Phys. Rev. E **83**, 051135 (2011); Chaos **21**, 047518 (2011).
[36] P. Kalinay and F. Slanina, Phys. Rev. E **104**, 064115 (2021).
[37] P. Kalinay, Phys. Rev. E **84**, 011118 (2011).
[38] R. L. Stratonovich, Radiotekh. Elektron. **3**, 497 (1958), in Russian.
[39] P. Reimann, C. Van den Broeck, H. Linke, P. Hänggi, J. M. Rubi, and A. Pérez-Madrid, Phys. Rev. E **65**, 031104 (2002).
[40] S. Lifson and J. L. Jackson, J. Chem. Phys. **36**, 2410 (1962).
[41] P. Kalinay and F. Slanina, J. Phys.: Condens. Matter **30**, 244002 (2018).
[42] K. Jain, R. Marathe, A. Chaudhuri, and A. Dhar, Phys. Rev. Lett. **99**, 190601 (2007).
[43] P. Kalinay, Phys. Rev. E **89**, 042123 (2014).
[44] R. Chatterjee, S. Chatterjee, P. Pradhan, and S. S. Manna, Phys. Rev. E **89**, 022138 (2014).